ELSEVIER

Development and application of a cubic eddy-viscosity model of turbulence

T. J. Craft, B. E. Launder, and K. Suga
Department of Mechanical Engineering, University of Manchester Institute of Science and Technology, Manchester, UK

Many quadratic stress–strain relations have been proposed in recent years to extend the applicability of linear eddy-viscosity models at modest computational cost. However, comparison shows that none achieves much greater width of applicability. This paper, therefore, proposes a cubic relation between the strain and vorticity tensor and the stress tensor, which does much better than a conventional eddy-viscosity scheme in capturing effects of streamline curvature over a range of flows. The flows considered range from simple shear at high strain rates and pipe flow, to flows involving strong streamline curvature and stagnation.

Keywords: turbulence model; nonlinear eddy-viscosity model; impinging flows; streamline curvature

Introduction

The rapid advance of computational schemes able, in principle, to analyse fluid flow and convective heat or mass transport over domains of arbitrary complexity again focuses attention on the method of characterizing turbulent exchange processes. The inadequacies of eddy-viscosity models in even mild departures from simple strain, which have been known and documented for over 20 years (Bradshaw 1973), are now brought into sharper relief as attention shifts to the far more complex flow fields that arise in the engineering environment.

Now, stress-transport models of turbulence offer a more reliable way of handling complex strain fields, but schemes of this type in fairly widespread use have been developed with the idea that any rigid surface can (as far as the turbulence is concerned) be regarded as infinite and plane. That constraint is inapplicable to the great majority of flows in the mechanical engineering sector that might use computational fluid dynamics (CFD) for their analysis. Quite apart from this serious deficiency, stress transport schemes are still regarded as requiring too much computer resource for industrial use, especially in three-dimensional (3-D) flows where all stress components are nonzero.

An alternative, much simpler route is available for approximating the Reynolds stresses which adopts an algebraic connection between stress and strain — albeit not a linear relationship. Such relationships may be arrived at by simplifying stress-transport models (so-called *algebraic* stress models, ASMs) but, in view of the current limitations of such schemes alluded to above, it is best to regard them simply as conjectured generalizations of the eddy-viscosity approach, containing quadratic and, occasionally, higher-order products of the strain and vorticity tensors. The earliest schemes go back to the 1970s (Pope 1975), although, in the last few years, there have been concerted efforts by many different groups world wide.

If we retain simply quadratic terms, the basic stress–strain relationship may be written as follows:

$$
\begin{aligned}
a_{ij} \equiv \frac{\overline{u_i u_j} - \frac{2}{3}\delta_{ij} k}{k}
&= -\frac{\nu_t}{k} S_{ij} + c_1 \frac{\nu_t}{\varepsilon}\left(S_{ik}S_{kj} - \frac{1}{3} S_{kl}S_{kl}\delta_{ij}\right) \\
&\quad + c_2 \frac{\nu_t}{\varepsilon}\left(\Omega_{ik}S_{kj} + \Omega_{jk}S_{ki}\right) \\
&\quad + c_3 \frac{\nu_t}{\varepsilon}\left(\Omega_{ik}\Omega_{jk} - \frac{1}{3}\Omega_{lk}\Omega_{lk}\delta_{ij}\right)
\end{aligned}
\tag{1}
$$

where

$$
S_{ij} = \left(\frac{\partial U_i}{\partial x_j} + \frac{\partial U_j}{\partial x_i}\right), \quad \Omega_{ij} = \left(\frac{\partial U_i}{\partial x_j} - \frac{\partial U_j}{\partial x_i}\right) - \varepsilon_{ijk}\Omega_k
$$

and Ω_k is the rotation rate of the coordinate system.

As presented, four empirical coefficients appear in Equation 1: c_μ, the usual coefficient found in linear schemes and the coefficients of the quadratic terms, $c_1 - c_3$. Table 1 shows the values proposed for these coefficients in a number of recent studies. * All of these studies arrived at the recommended coefficient values by considering the prediction of shear stress in a simple shear and one other complex flow (or some other feature of a simple shear — such as the normal stress level — that cannot be mimicked with a linear scheme). Evidently, in arriving at the respective optimized sets, very different values have

Address reprint requests to Prof. B. E. Launder, Mechanical Engineering Department, UMIST, P.O. Box 88, Manchester M601QD, UK.

Received 24 January 1995; accepted 9 August 1995

Int. J. Heat and Fluid Flow 17: 108–115, 1996

655 Avenue of the Americas, New York, NY 10010

* The quantities S and Ω appearing in the model of Shih et al. (1993) are dimensionless strain rates and vorticities and appear again later.

0142-727X/96/$15.00
SSDI 0142-727X(95)00079-8

Table 1 Earlier constitutive relations based on Equation 1

Model	c_μ	c_1	c_2	c_3	Additional terms
Speziale (1987)	0.09	−0.15	0.00	0.00	$-0.3\ \nu_t/\varepsilon\ (\dot{S}_{ij} - 1/3\ \dot{S}_{kk}\ \delta_{ij})$
Nisizima and Yoshizawa (1987)	0.09	−0.76	0.18	1.04	
Rubinstein and Barton (1990)	0.0845	0.68	0.14	−0.56	
Myong and Kasagi (1990)	0.09	0.28	0.24	0.05	W_{ij}
Shih, Zhu and Lumley (1993)	$\dfrac{2/3}{1.25 + S + 0.9\Omega}$	$\dfrac{0.75/c\mu}{1000 + S^3}$	$\dfrac{3.8/c\mu}{1000 + S^3}$	$\dfrac{4.8/c\mu}{1000 + S^3}$	

$$\dot{S}_{ij} = \frac{\partial S_{ij}}{\partial t} + U_k \frac{\partial S_{ij}}{\partial x_k} - \frac{\partial U_i}{\partial x_k} S_{kj} - \frac{\partial U_j}{\partial x_k} S_{ki}$$

$$W_{ij} = \frac{2}{3}\frac{\nu}{\varepsilon}\left(\frac{\partial\sqrt{k}}{\partial x_n}\right)^2 (-\delta_{ij} - \delta_{in}\delta_{jn} + 4\delta_{im}\delta_{jm})$$

(n and m denote wall-normal and streamwise direction)

emerged for the coefficients $c_1 - c_3$ depending on what flow or flow feature was chosen to predict. This seems to indicate that, at quadratic level, only slightly greater generality is achievable than with the usual linear eddy-viscosity model. In particular, the various effects of streamline curvature on the turbulent stresses cannot be adequately accounted for at this level.

This realization has shaped the strategy of the present contribution. A cubic stress–strain relation has been adopted here; the greater flexibility that this has brought enables stress levels to be captured over a far wider range of complex strain fields than hitherto. A preliminary version of this model was reported at the 5th Symposium on Refined Flow Modelling and Turbulence Measurement (Craft et al. 1993). The model coefficients have, however, been entirely retuned since that study for the present archival contribution.

Proposed model

Stress–strain relationship

In the Introduction section, we reported that the numerous proposals for quadratic stress–strain relationships showed little width of applicability. Here, therefore, efforts have been focused on providing a suitable cubic stress–strain relation. The most general such expression retaining terms up to cubic level that satisfies the

Notation

a_{ij}	Reynolds stress anisotropy tensor $= \overline{u_i u_j}/k - 2/3\delta_{ij}$
D	pipe diameter
E	source term in $\tilde{\varepsilon}$ equation
h	channel width
H	height of impinging jet discharge above plate
k	Turbulent kinetic energy $= 1/2\overline{u_i u_i}$
Nu	Nusselt number
P_k	production rate of k
Pr	Prandtl number
r	radial distance
$R_1 R_2$	inner and outer radii of curved channel
Re	Reynolds number
R_t	turbulent Reynolds number
S	nondimensional strain rate $= k/\varepsilon\sqrt{(1/2 S_{ij} S_{ij})}$
$\tilde{S}$	nondimensional strain rate $= k/\tilde{\varepsilon}\sqrt{(1/2 S_{ij} S_{ij})}$
S_{ij}	mean strain rate tensor
u', v', w'	rms fluctuating velocities
$\overline{u_i u_j}$	Reynolds stress tensor
u_τ	wall friction velocity
U_b	bulk velocity
U_{cl}	centerline velocity
U_i, U, V, W	mean velocity components
U_{max}	maximum velocity
$W_{0.8}$	swirl velocity at $r/D = 0.4$
x_i	Cartesian coordinates
y	distance from wall
Y_c	Yap length scale correction

Greek

δ_{ij}	Kronecker delta
ε	dissipation rate of k
$\tilde{\varepsilon}$	"isotropic" dissipation rate, $\varepsilon - 2\nu(\partial k^{1/2}/\partial x_j)^2$
ε_{ijk}	alternating tensor
ν	kinematic viscosity
ν_t	turbulent viscosity
Ω	nondimensional vorticity $= k/\varepsilon\sqrt{(1/2\Omega_{ij}\Omega_{ij})}$
Ω_{ij}	mean vorticity tensor
Ω_k	rotation vector of coordinate system

required symmetry and contraction properties, can be written as follows:

$$
\begin{aligned}
a_{ij} = & -\frac{\nu_t}{k}S_{ij} + c_1\frac{\nu_t}{\tilde{\varepsilon}}\left(S_{ik}S_{jk} - 1/3S_{kl}S_{kl}\delta_{ij}\right) \\
& + c_2\frac{\nu_t}{\tilde{\varepsilon}}\left(\Omega_{ik}S_{jk} + \Omega_{jk}S_{ik}\right) \\
& + c_3\frac{\nu_t}{\tilde{\varepsilon}}\left(\Omega_{ik}\Omega_{jk} - 1/3\Omega_{kl}\Omega_{kl}\delta_{ij}\right) \\
& + c_4\frac{\nu_t k}{\tilde{\varepsilon}^2}\left(S_{ki}\Omega_{lj} + S_{kj}Q_{li}\right)S_{kl} \\
& + c_5\frac{\nu_t k}{\tilde{\varepsilon}^2}\left(\Omega_{il}\Omega_{lm}S_{mj} + S_{il}\Omega_{lm}\Omega_{mj} - \tfrac{2}{3}S_{lm}\Omega_{mn}\Omega_{nl}\delta_{ij}\right) \\
& + c_6\frac{\nu_1 k}{\tilde{\varepsilon}^2}S_{ij}S_{kl}S_{kl} + c_7\frac{\nu_t k}{\tilde{\varepsilon}^2}S_{ij}\Omega_{kl}\Omega_{kl}
\end{aligned}
\tag{2}
$$

Besides the indicated role of the stress and vorticity tensors, the dimensionless strain and vorticity invariants

$$
\tilde{S} \equiv \frac{k}{\tilde{\varepsilon}}\sqrt{1/2S_{ij}S_{ij}} \qquad \tilde{\Omega} \equiv \frac{k}{\tilde{\varepsilon}}\sqrt{1/2\Omega_{ij}\Omega_{ij}} \tag{3}
$$

are introduced as parameters. The turbulent viscosity $\nu_t = c_\mu f_\mu k^2/\tilde{\varepsilon}$, where $\tilde{\varepsilon}$ is the so-called isotropic dissipation (Jones and Launder 1972), $\varepsilon - 2\nu\ (\partial k^{1/2}/\partial x_j)^2$, a quantity that vanishes at the wall.

Lee et al. (1990), from a comparative DNS study of the appearance of eddy structures in homogeneous shear flows and near-wall turbulence, concluded that it was really the strain invariant that was mainly responsible for the streaky structure found in the viscous "buffer" region near a wall rather than the turbulent Reynolds number. Our own turbulence model explorations, as those of our colleagues (Cotton and Ismael 1993), confirm that conclusion; namely, that the near-wall behavior of turbulence, although strongly affected by viscosity, cannot be adequately characterized in terms of a single viscosity-based parameter. The strain parameter, S, provides a possible additional parameter.

Optimization over a wide range of flows, described later, has resulted in the following expressions for c_μ and f_μ:

$$
c_\mu = \frac{0.3}{1 + 0.35\left(\max(\tilde{S}, \tilde{\Omega})\right)^{1.5}} \times \left(1 - \exp\left[\frac{-0.36}{\exp\left(-0.75\max(\tilde{S}, \tilde{\Omega})\right)}\right]\right)
$$

$$
f_\mu = 1 - \exp\left[-(R_t/90)^{1/2} - (R_t/400)^2\right]
$$

where $R_t \equiv k^2/\nu\tilde{\varepsilon}$ and the coefficients $c_1, \ldots, c_7$ are given in Table 2.

In a simple shear flow, the choice $c_6 = -c_7$ results in the linear term being the only contribution to the shear stress (i.e., $a_{12} = -(\nu_t/k)\,\mathrm{d}U_1/\mathrm{d}x_2$). The functional form of c_μ has thus been tuned so that, in a simple homogeneous shear flow at high Reynolds number, good agreement with experimental and direct numerical simulation data is obtained for the variation of $\overline{uv}/k$ with strain rate S, as shown in Figure 1. The nonlinear elements allow good predictions to be obtained also for the normal stress anisotropies. Note that the linear eddy-viscosity model gives $a_{11} = a_{22} = 0$, and $a_{12} = -0.09\ S$. The quadratic models, summarized in Table 1, also fail to predict the correct variation of a_{ij} with S in this simple shear flow.

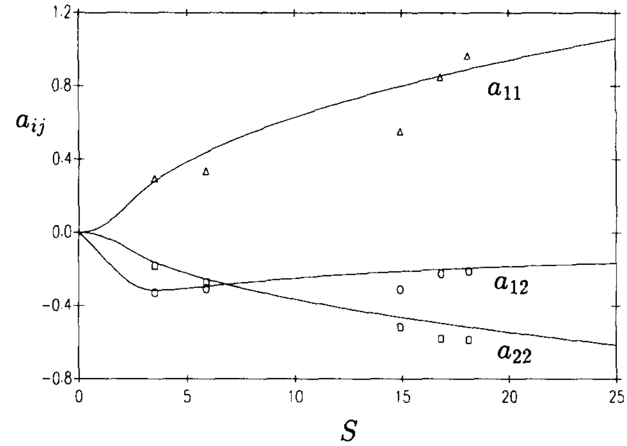

Figure 1 Variation of stress anisotropies with strain rate in high Reynolds number homogeneous shear flow (symbols: DNS data of Lee et al. (1990) (S = 15–18) and experiments of Champagne et al. (1970), and Tavoularis and Corrsin (1981) (S = 3.5, 6); lines present predictions)

An additional Reynolds number-dependent damping term f_μ is still required for near-wall flows, but its influence is considerably less than that used in the linear eddy-viscosity models, because now a substantial amount of the near-wall strain-related damping is provided by the functional form of c_μ.

Dissipation rate modeling

The turbulence energy k and its "isotropic" dissipation rate $\tilde{\varepsilon}$ are obtained from the transport equations:

$$
\frac{Dk}{Dt} = P_k - \varepsilon + \frac{\partial}{\partial x_j}\left[(\nu + \nu_t/\sigma_\kappa)\frac{\partial k}{\partial x_j}\right]
$$

$$
\frac{D\tilde{\varepsilon}}{Dt} = c_{\varepsilon 1}\frac{\tilde{\varepsilon}}{k}P_k - c_{\varepsilon 2}\frac{\tilde{\varepsilon}^2}{k} + E + Y_c + \frac{\partial}{\partial x_j}\left[(\nu + \nu_t/\sigma_\varepsilon)\frac{\partial\tilde{\varepsilon}}{\partial x_j}\right] \tag{4}
$$

where

$$
P_k = -\overline{u_i u_j}\frac{\partial U_i}{\partial x_j}\ ;\ \varepsilon = \tilde{\varepsilon} + 2\nu\left(\frac{\partial\sqrt{k}}{\partial x_j}\right)^2 \tag{5}
$$

and the various coefficients are given in Table 3.

Table 2 The proposed form for the coefficients of Equation 2

c_1	c_2	c_3	c_4	c_5	c_6	c_7
−0.1	0.1	0.26	$-10\ c_\mu^2$	0	$-5\ c_\mu^2$	$5c_\mu^2$

Table 3 Coefficients in k and $\tilde{\varepsilon}$ equations

$c_{\varepsilon 1}$	$c_{\varepsilon 2}$	σ_k	σ_ε
1.44	$1.92\ (1\text{-}0.3\ \exp(-R_t^2))$	1.0	1.3

The near-wall source term E, which in the Launder–Sharma (1974) model, takes the form $2\nu\nu_t(\partial^2 U_i/\partial x_j \partial x_k)^2$, is here modified to reduce its dependence on Reynolds number. Consequently, it is modeled as follows:

$$E = 0.0022 \frac{\tilde{S}\nu_t k^2}{\tilde{\varepsilon}} \left(\frac{\partial^2 U_i}{\partial x_j \partial x_k} \right)^2 \quad \text{for } R_t \leq 250 \tag{6}$$

The Yap (1987) length-scale correction Y_c, which is normally employed in the linear k-ε model, is retained here also. It can be written as follows:

$$Y_c = \max\left(0.83 \frac{\tilde{\varepsilon}^2}{k} \left[\frac{k^{1.5}}{2.5\tilde{\varepsilon} y} - 1 \right] \left[\frac{k^{1.5}}{2.5\tilde{\varepsilon} y} \right]^2, 0 \right) \tag{7}$$

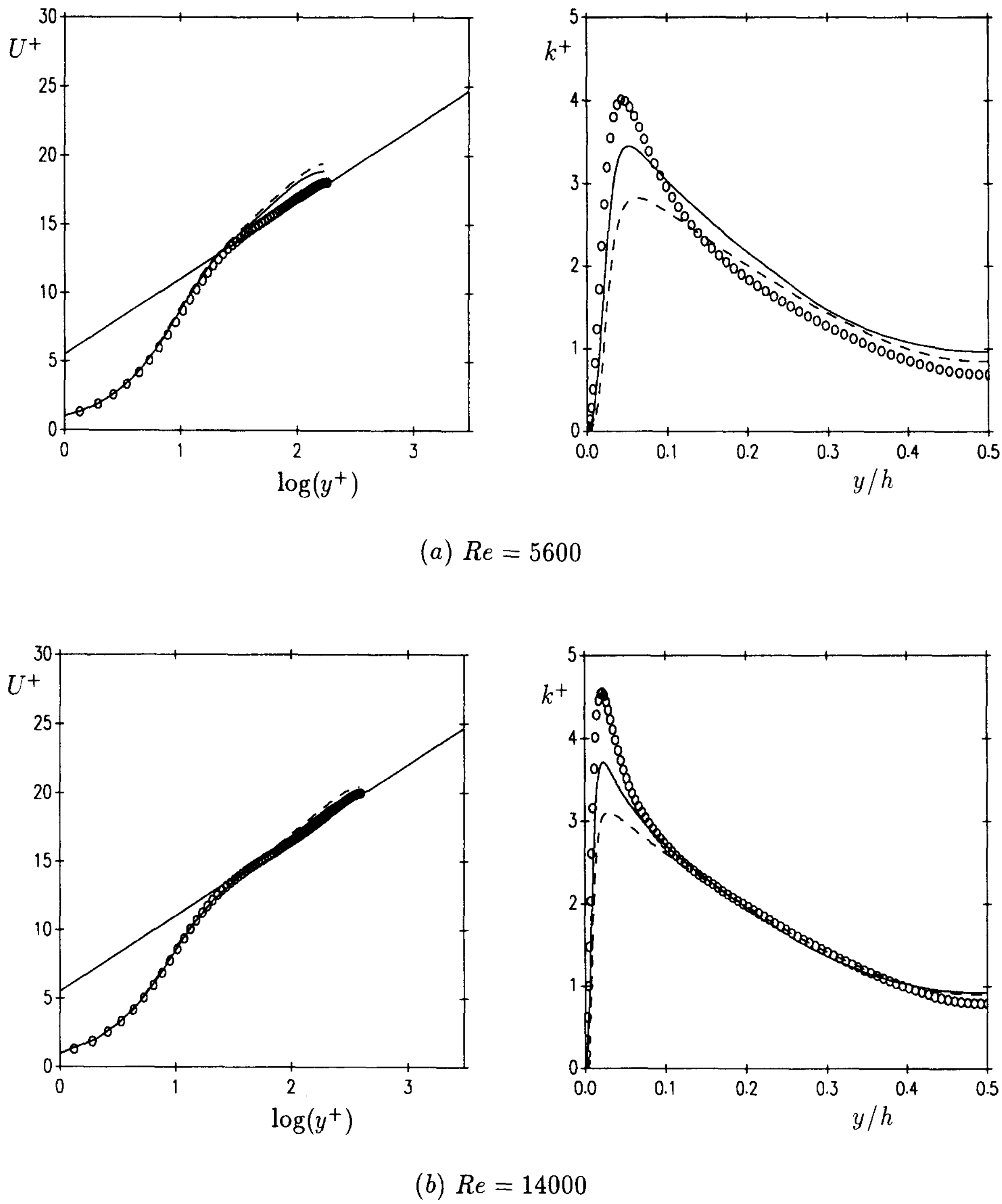

Figure 2 Profiles of mean velocity and turbulence energy in plane channel flow at Reynolds number of 5600 and 14,000; _____ present model; _ _ _ _ _ Launder and Sharma (1974); ∘ DNS, Kim et al. (1987); Kim (personal communication 1989)

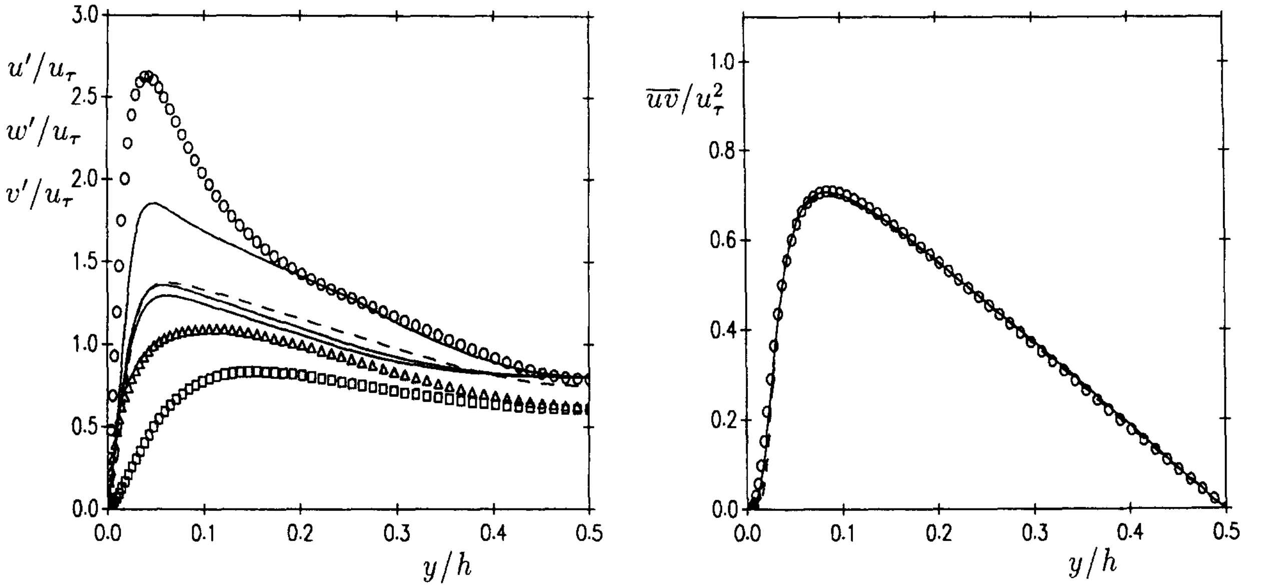

Figure 3 Reynolds stresses in plane channel flow at Re = 5600; _____ present model; _ _ _ _ _ Launder and Sharma (1974); symbols DNS, Kim et al. (1987)

where y is the distance to the wall. The role of this term is to reduce the otherwise excessive levels of length scale in the near-wall region of separated and stagnating flows.

Applications of the model

The first test case considered is a plane channel flow. Figure 2 shows predictions of mean velocity and turbulence energy with direct simulation data at bulk Reynolds numbers of 5600 and 14,000. The current predictions are generally closer to the data than with the Launder–Sharma (1974) model, which fails to capture the near-wall peak in k.

It is only the shear stress which affects the mean velocity in this simple shear flow, and from Figure 3 this can be seen to be very well predicted. Although (unlike any linear eddy-viscosity scheme) the present model does give a separation between the normal stress components, the difference is not as large as is found in the direct numerical simulation (DNS) data, particularly in the near-wall region. Although this certainly is a deficiency, it is not, we suggest, a terribly serious one, because in this immediate near-wall region, it is the shear stress that governs the mean flow behaviour. Of course, in the limit, where we consider perpendicular flow impingement, the normal stresses *must* be influential. As shown later, however, in this limit, very satisfactory normal-stress profiles are obtained.

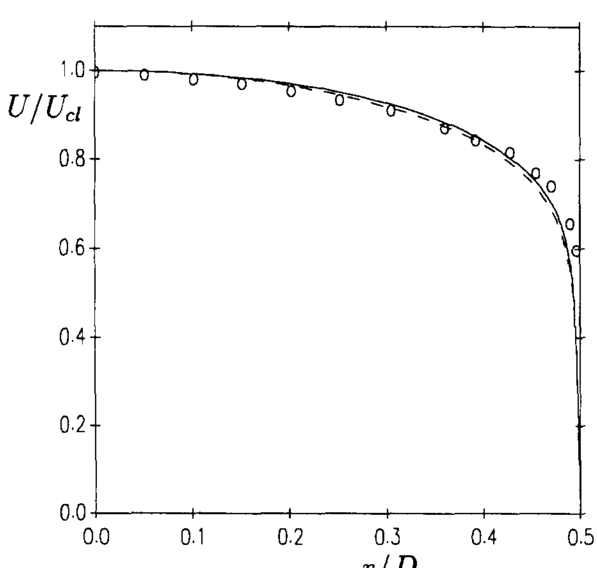

Figure 4 Mean velocity profile in circular pipe flow at Re = 45,000; _____ present model; _ _ _ _ _ Launder and Sharma (1974); ○ Laufer (1954)

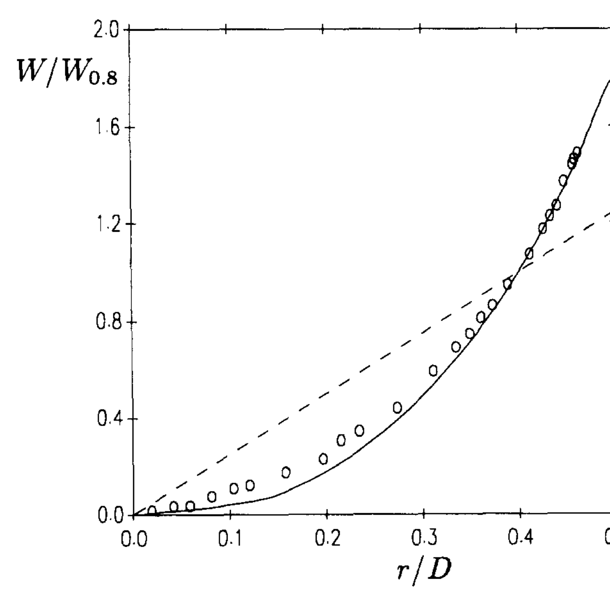

Figure 5 Swirl velocity profile in a pipe rotating about its own axis (Re = 45,000); _____ present model; _ _ _ _ _ Launder and Sharma (1974); ○ Cheah et al. (1993)

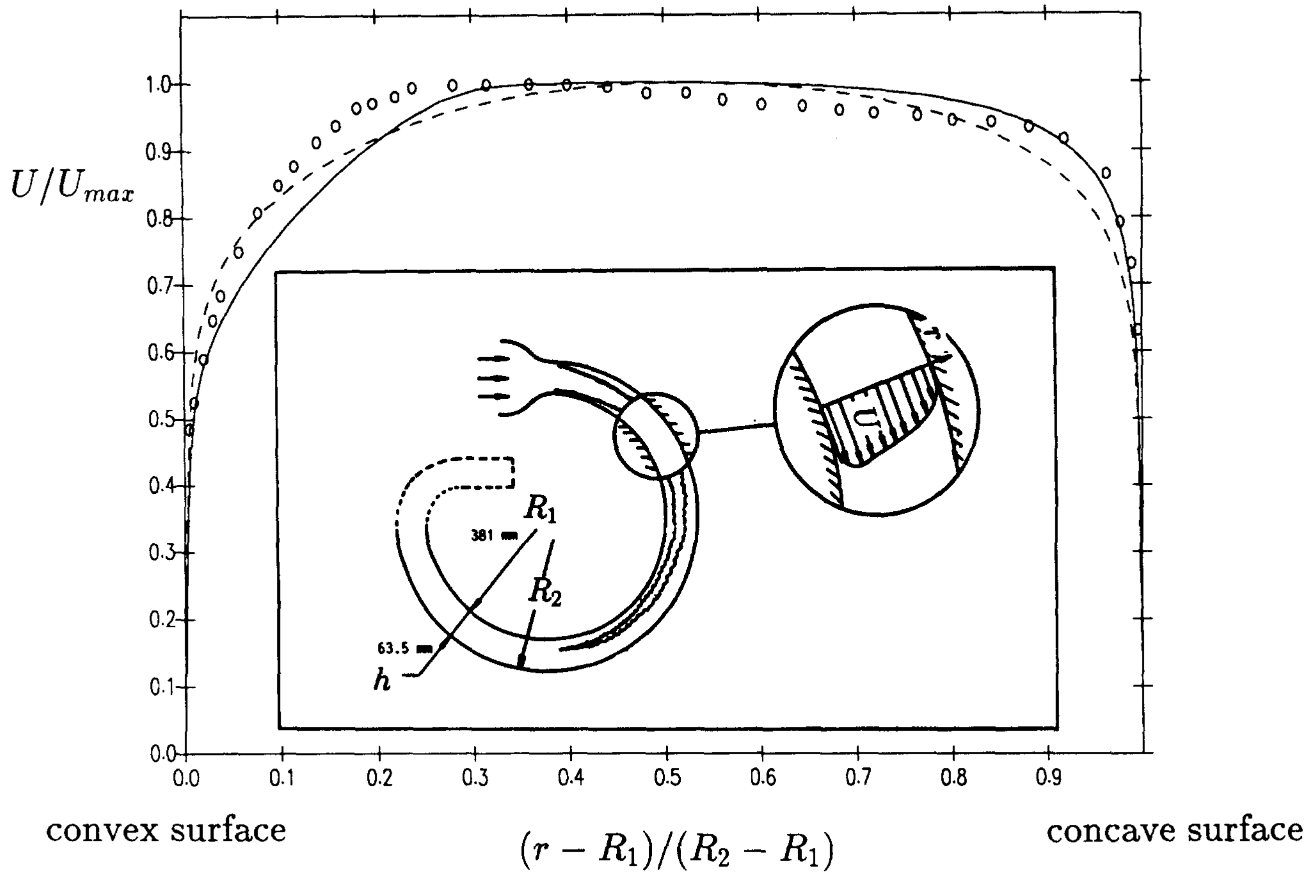

Figure 6 Mean velocity profile in fully developed curved channel flow at Re = 70,000; _____ present model; _ _ _ _ _ Launder and Sharma (1974); ○ Ellis and Joubert (1974)

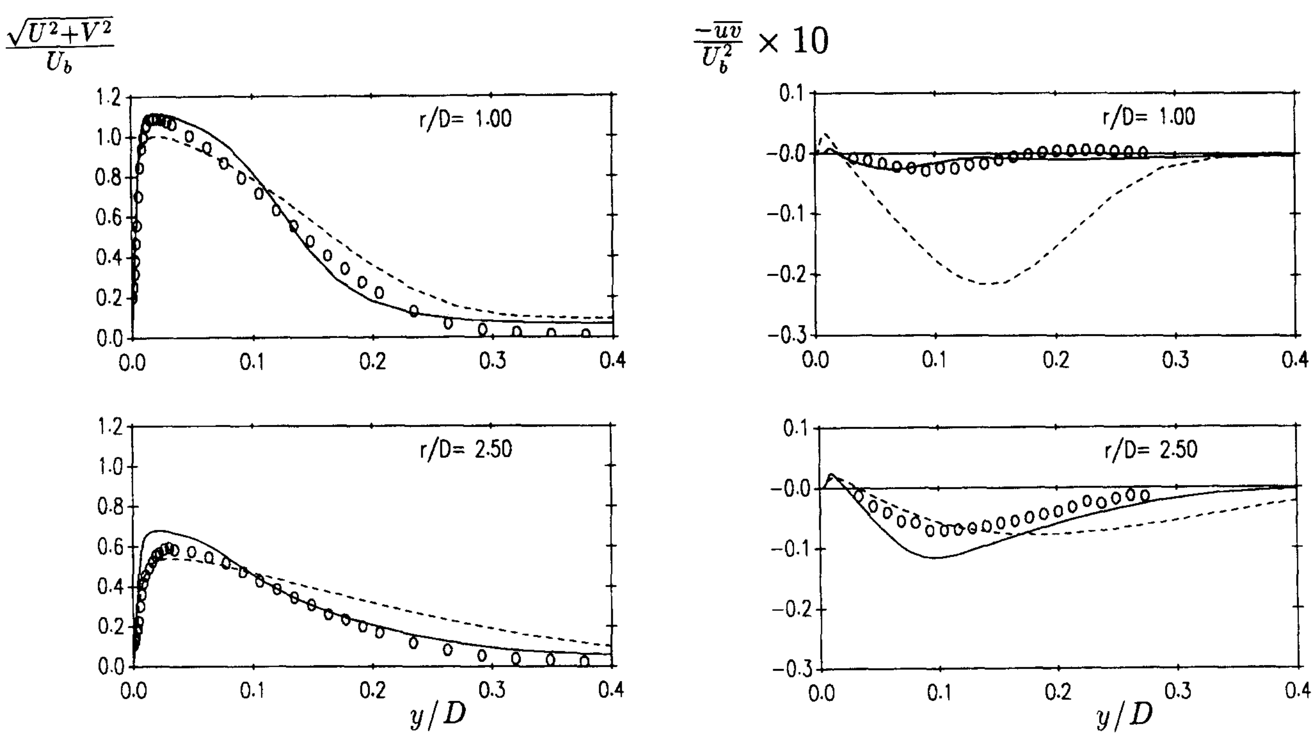

Figure 7 Profiles of mean velocity and shear stress at radial distances $r/D = 1$ and 2.5 in the impinging jet with $H/D = 2$ and Re = 23,000; _____ present model; _ _ _ _ _ Launder and Sharma (1974); ○ Cooper et al. (1993)

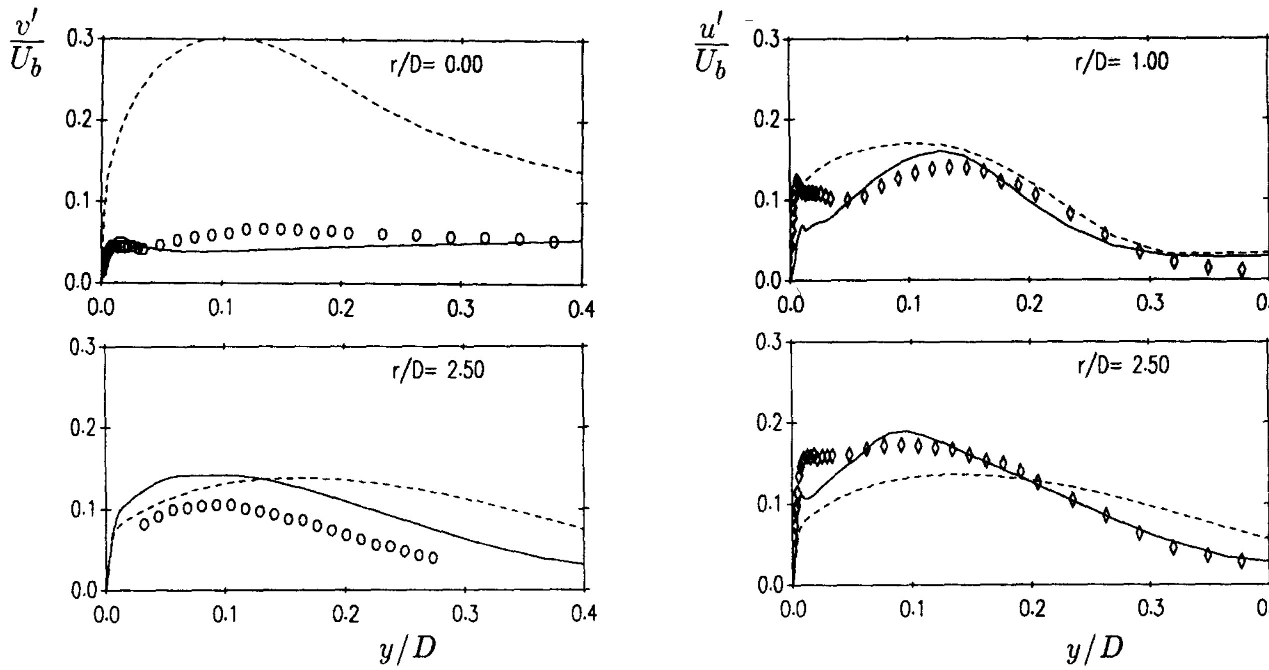

Figure 8 Profiles of rms velocities perpendicular (v) and parallel (u) to the wall in the impinging jet; _____ present model; _ _ _ _ _ Launder and Sharma (1974); symbols, Cooper et al. (1993)

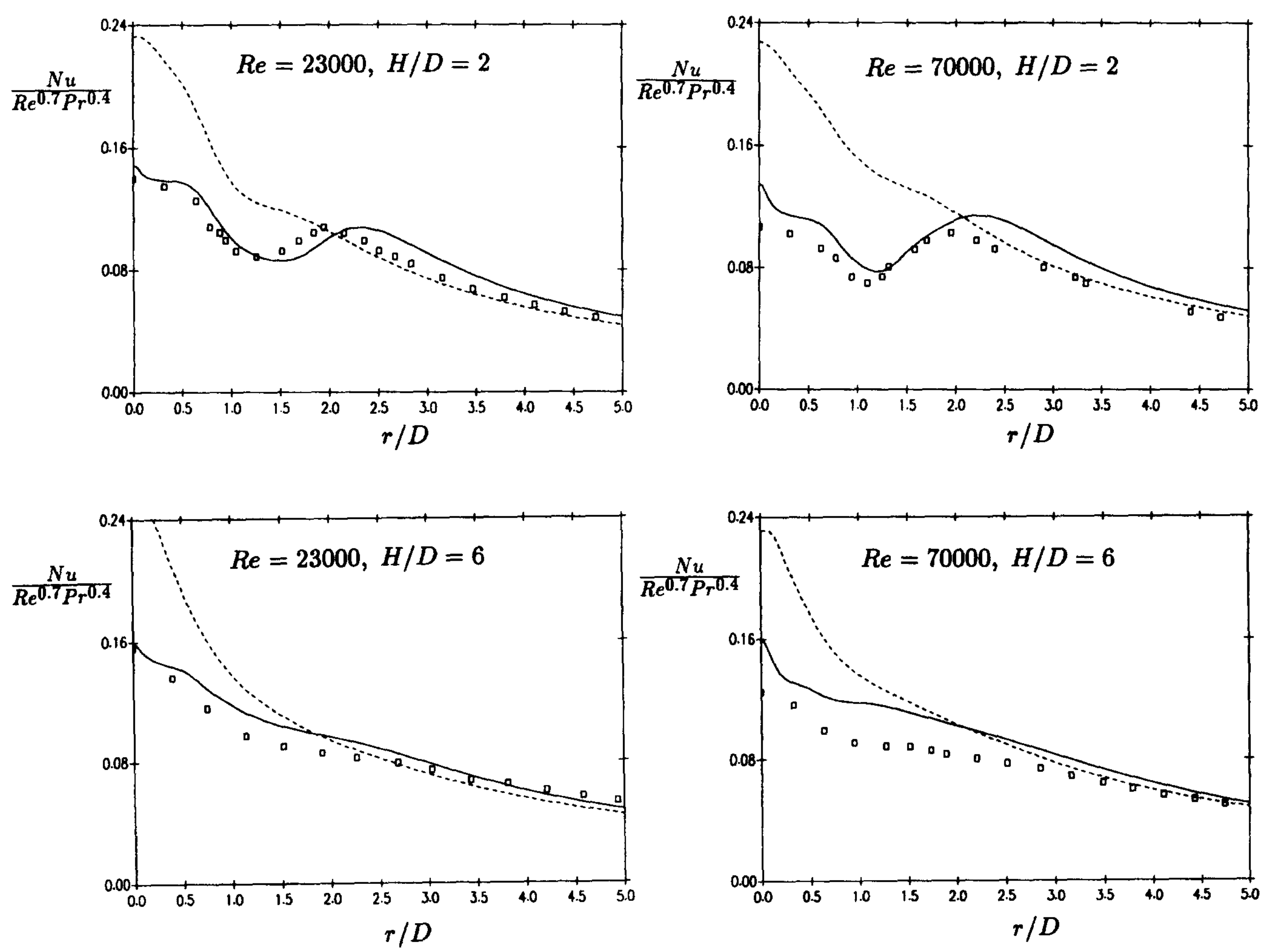

Figure 9 Nusselt number distributions in the impinging jet cases; _____ present model; _ _ _ _ _ Launder and Sharma (1974); □ Baughn and Shimizu (1989), Baughn et al. (1992)

Figure 4 compares the mean velocity profile across a circular pipe with Laufer's (1954) experimental data. Both the present model and the Launder–Sharma (1974) model give predictions close to the data. A very marked difference does, however, arise in the case when the pipe rotates about its own axis (Figure 5). In this case, any linear eddy-viscosity scheme would predict a linear variation of circumferential mean velocity with radius: whereas, the present model returns a strongly nonlinear increase, in line with the experimental data (Cheah et al. 1993).

To assess the model's prediction of streamline curvature effects, Figure 6 shows predictions of the mean velocity profile in a fully developed curved channel flow studied experimentally by Ellis and Joubert (1974). The curvature leads to increased mixing near the concave surface and damping near the convex wall, resulting in a strongly asymmetric velocity profile with the shear stress on the inner wall being barely 40% of that on the outer. In this case, the present model does create an asymmetry in the profile of the correct sense, and returns a shear stress ratio on the two walls of about 60% compared with nearly 90% in the case of the linear eddy-viscosity model.

The final test case is a round, turbulent jet impinging normally onto a heated flat plate. The thermal field measurements are from Baughn and Shimizu (1989), and the corresponding velocity field has been documented by Cooper et al. (1993). Configurations have been computed with discharge heights of 2 and 6 jet diameters above the plate surface and at Reynolds numbers of 23,000 and 70,000. Impinging jets offer one of the most difficult classes of flow to predict, because on both the symmetry axis and in the region of strong streamline curvature induced by the wall, the deformation tensor is very different from that of a simple shear for which most models have been calibrated. Figures 7 and 8 show mean velocity, shear stress, and normal stress profiles, plotted against distance from the wall, at various radial positions for the case of $H/D = 2$, at $\mathrm{Re} = 23{,}000$. The considerable improvements the present model brings to the stress field, particularly in the impingement zone, result in the mean velocity peaks being more accurately captured. The same improvements in the dynamic field are also found at the higher Reynolds number and discharge height. The heat-transfer for the impinging jet case has been computed by prescribing a constant turbulent Prandtl number of 0.9, the usually prescribed value for near-wall turbulence. Figure 9 shows the Nusselt number distributions at both Reynolds numbers and discharge heights. The low levels of turbulence energy predicted by the present model in the impingement zone results in much improved heat transfer levels, although at the higher Reynolds number, there is still a small peak at the stagnation point, which is not found experimentally.

Conclusions

This paper introduced a new nonlinear model in which strain and vorticity tensors to cubic level are retained. Comparisons over a range of complex shear flows have shown that the model performs consistently better than a linear eddy-viscosity scheme. As a final point, it must be emphasized that computing times required for this type of closure are typically only 10% more than for a linear EVM. Thus, it seems ideally suited for inclusion in commercial software.

Acknowledgments

Different aspects of the project have been sponsored by the UK SERC, Rolls Royce plc, and Toyota Central R & D laboratories. Authors' names are listed alphabetically.

References

Baughn, J. W. and Shimizu, S. 1989. Heat transfer measurements from a surface with uniform heat flux and an impinging jet. *J. Heat Transfer*, **111**, 1096–1098

Baughn, J. W., Yan, X. J. and Mesbah, M. 1992. The effect of Reynolds number on the heat transfer distribution from a flat plate to a turbulent impinging jet. *Proc. ASME Winter Annual Meeting*

Bradshaw, P. 1973. The effects of streamline curvature on turbulent flow. AGARDograph 169

Champagne, F. H., Harris, V. G. and Corrsin, S. 1970. Experiments on nearly homogeneous turbulent shear flow. *J. Fluid Mech.*, **41**, 81–139

Cheah, S. C., Cheng, L., Cooper, D. and Launder, B. E. 1993. On the structure of turbulent flow in spirally fluted tubes. *Proc. 5th Int. Symp. Refined Flow Modeling and Turbulence Measurements*, Paris

Cooper, D., Jackson, D. C., Launder, B. E. and Liao, G. X. 1993. Impinging jet studies for turbulence model assessment, Part 1: Flow field measurements. *Int. J. Heat Mass Transfer*, **36**, 2675–2684

Cotton, M. A. and Ismael, J. O. 1993. Development of a two-equation turbulence model with reference to a strain parameter. *Proc. 5th Int. Symp. Refined Flow Modeling and Turbulence Measurements*, Paris

Craft, T. J., Launder, B. E. and Suga, K. 1993. Extending the applicability of eddy-viscosity models through tie use of deformation invariants and nonlinear elements. *Proc. 5th Int. Symp. Refined Flow Modeling and Turbulence Measurements*, Paris

Ellis, L. B. and Joubert, P. N. 1974. Turbulent shear flow in a curved duct. *J. Flid Mech.*, **62**, 65–84

Jones, W. P. and Launder, B. E. 1972. Some properties of sink-flow turbulent boundary layers. *J. Fluid Mech.*, **56**, 337–351

Kim, J., Moin, P. and Moser, R. 1987. Turbulence statistics in fully developed channel flow at low Reynolds number. *J. Fluid Mech.*, **177**, 133–166

Laufer, J. 1954. The structure of turbulence in fully developed pipe flow. NACA report 1174

Launder, B. E. and Sharma, B. I. 1974. Application of the energy-dissipation model of turbulence to the calculation of flow near a spinning disc. *Lett. Heat Mass Transfer*, **1**, 131–138

Lee, M. J., Kim, J. and Moin, P. 1990. Structure of turbulence at high shear rate. *J. Fluid Mech.* **216**, 561–583

Myong, H. K. and Kasagi, N. 1990. Prediction of anisotropy of the near wall turbulence with an anisotropic low-Reynolds-number k-ε turbulence model. *J. Fluids Eng.*, **112**, 521–524

Nisizima, S. and Yoshizawa, A. 1987. Turbulent channel and Couette flows using an anisotropic k-ε model. *AIAA J.*, **25**, 414–420

Pope, S. 1975. A more general effective-viscosity hypothesis. *J. Fluid Mech.*, **72**, 331–340

Rubinstein, R. and Barton, J. M. 1990. Non-linear Reynolds stress models and renormalization group. *Phys. Fluids*, **A2**, 1472–1476

Shih, T. H., Zhu, J. and Lumley, J. L. 1993. A realizable Reynolds stress algebraic equation model. NASA tech. memo. 105993

Speziale, C. G., 1987. On non-linear k-l and k-ε models of turbulence. *J. Fluid Mech.*, **178**, 459–475

Tavoularis, S. and Corrsin, S. 1981. Experiments in nearly homogeneous turbulent shear flow with a uniform mean temperature gradient, Part 1. *J. Fluid Mech.*, **104**, 311–347

Yap, C. R. 1987. Turbulent heat and momentum transfer in recirculating and impinging flows. Ph.D. thesis, Faculty of Technology, University of Manchester, Manchester, UK